

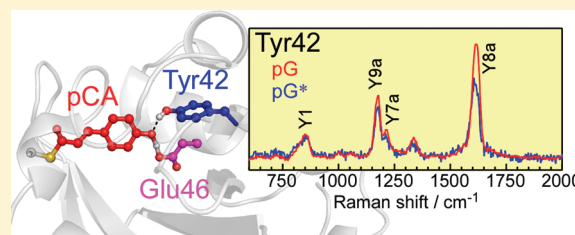
Changes in the Hydrogen-Bond Network around the Chromophore of Photoactive Yellow Protein in the Ground and Excited States

Misao Mizuno,[†] Hironari Kamikubo,[‡] Mikio Kataoka,[‡] and Yasuhisa Mizutani^{*,†}

[†]Department of Chemistry, Graduate School of Science, Osaka University, 1-1 Machikaneyama, Toyonaka, Osaka 560-0043, Japan

[‡]Graduate School of Materials Science, Nara Institute of Science and Technology, 8916-5 Takayama, Ikoma, Nara 630-0192, Japan

ABSTRACT: Changes in the hydrogen-bond (HB) network around the chromophore, *p*-coumaric acid (pCA), in the ground pG and excited pG* states were investigated for wild type (WT) photoactive yellow protein (PYP) and its mutants using ultraviolet resonance Raman (UVR) spectroscopy. The intensity depletion of Tyr UVR bands was observed upon photoexcitation of pCA to the pG* state. The spectral change was ascribed to strengthening of HB between pCA and Tyr42. Comparison of Raman intensities indicated that, in the pG state, the HB between pCA and Tyr42 in WT is a short HB, which is weaker than that in E46Q mutant. In the pG* state, the HB network around pCA of WT is similar to that of E46Q mutant. The present results demonstrate that the HB between pCA and Tyr42 and that between pCA and Glu46 are correlated with each other in the HB network.



Photoactive yellow protein (PYP) is a putative blue-light sensor that controls the phototaxis of a bacterium, *Halorhodospira halophila*.¹ The chromophore of PYP is *p*-coumaric acid (pCA), which is buried in a hydrophobic pocket. After pCA in the ground pG state is photoexcited to the pG* state, trans \rightarrow cis isomerization leads to a cyclic reaction involving a series of ground-state intermediate states, noted as I_0 , I_0^+ , pR, and pB.^{2,3} The I_0 and I_0^+ intermediates are the early red-shifted states with similar absorption properties. After a few nanoseconds, I_0^+ thermally relaxes to the pR intermediate (also referred to as I_1 or PYP_L), which finally converts on a submillisecond time scale to a signaling state of PYP called pB (also referred to as I_2 or PYP_M). In the photocycle, the rearrangement of the hydrogen-bond (HB) network around pCA plays a crucial role in facilitating signal transduction. In the pG state, short HBs (SHBs) are formed between pCA and Glu46 as well as between pCA and Tyr42.⁴ Recently, high-resolution neutron crystallographic analysis has revealed a difference between the two SHBs.⁵ The hydrogen atom between pCA and Glu46 locates in the middle between the phenolic oxygen of pCA and the carboxylate oxygen of Glu46 and forms a covalent bond to neither oxygen atom. On the other hand, the hydrogen atom between pCA and Tyr42 forms a covalent bond to the phenolic oxygen of Tyr42. Thus, the SHB between pCA and Glu46 is categorized to a low-barrier HB (LBHB), whereas the SHB between pCA and Tyr42 is not a LBHB.

Ultraviolet resonance Raman (UVR) spectroscopy selectively enhances the vibrational Raman bands of aromatic amino acid side chains, such as Tyr and Trp, thereby allowing specific sites in protein structures to be probed. Using picosecond time-resolved UVR spectroscopy, we determined that structural changes in Tyr residue(s) are associated with the photoreaction

of pCA.⁶ In the present paper, we identify the Tyr residue responsible for these changes in the UVR spectra in the picosecond region based on measurements on mutant PYP. We also investigate changes in the HB network around pCA in the pG and pG* states.

EXPERIMENTAL SECTION

Sample Preparation. The WT, E46Q, and Y42F PYP were prepared as described previously.⁷ The sample was dissolved in 10 mM Tris-HCl buffer at pH 7.0. For time-resolved UVR measurements, the sample concentration was 100 μ M. For steady-state UVR measurements, the sample concentrations of WT, E46Q, and Y42F PYP were 100, 90, and 70 μ M, respectively.

Time-Resolved Measurements Using Picosecond Laser Pulses. The experimental setup for picosecond time-resolved UVR measurements has been described elsewhere.^{6,8} Briefly, the light source of our apparatus was a picosecond Ti:sapphire oscillator (Tsunami pumped by Millennia-Vs, Spectra-Physics) and amplifier (Spitfire pumped by Evolution-15, Spectra-Physics) system operating at 1 kHz. The wavelength and energy of the laser output were 789 nm and 800 μ J, respectively. To generate the pump and probe pulses, the second harmonic of the laser output was divided into two parts. The pump arm contained a Raman shifter with compressed CH₄ gas. The pump pulse, 446 nm, was the first Stokes line generated from the Raman shifter. The probe arm contained a Raman shifter with compressed H₂ gas.

Received: March 29, 2011

Revised: June 16, 2011

Published: June 17, 2011

The probe pulse, 236 nm, was the second harmonic of the first Stokes line generated from the Raman shifter and was introduced into an etalon to reduce the spectral width. The spectral width of the probe pulse was reduced to about 20 cm^{-1} . The pump and probe pulses were collinearly overlapped and focused onto a flowing thin film of the sample solution formed by a wire-guided jet nozzle.⁹ The sample solution was continuously flowed to ensure that every 1 kHz pulse hit a fresh portion of the solution. Typical pulse energy of the probe light was $0.5\text{ }\mu\text{J}$ ($0.71 \times 10^{-3}\text{ J/cm}^2$) at the sample point. Pulse energies of the pump light were $5\text{ }\mu\text{J}$ ($2.6 \times 10^{-3}\text{ J/cm}^2$) and $25\text{ }\mu\text{J}$ ($1.3 \times 10^{-2}\text{ J/cm}^2$) when measuring the spectra in Figures 1 and 3, respectively. The zero-delay time was precisely determined by measuring the intensity of the difference frequency generation between the pump and probe pulses. Typical cross-correlation time between the pump and probe pulses was 3.7 ps. The Raman scattering light was collected and focused onto the entrance slit of a homemade Czerny-Turner configured Littrow prism prefilter¹⁰ coupled to a 50 cm single spectrograph (500M, SPEX) by two achromatic doublet lenses. The dispersed light was detected with a liquid nitrogen cooled CCD camera (SPEC-10:400B/LN, Roper Scientific). The Raman shifts were calibrated with Raman bands of cyclohexane. The spectral dispersion was $3.0\text{--}3.5\text{ cm}^{-1}/\text{pixel}$ on the CCD camera. The accumulation times for obtaining the time-resolved spectra of WT and Y42F in Figure 1 were 68 and 40 min, respectively. The accumulation time for obtaining the spectra in Figure 3 was 90 min.

Steady-State Measurements Using Nanosecond Laser Pulses. The light source of the steady-state UVRr measurements was a Ti:sapphire laser pumped by a Q-switched LD-pumped Nd:YLF laser (DM laser system, Photonics Industries) operating at 1 kHz. The fourth harmonic of the laser output, 236 nm, was used as the probe light. The spectral width of the probe pulse was 8 cm^{-1} . Typical pulse energy and width of the probe light were $0.5\text{ }\mu\text{J}$ and 20 ns, respectively, at the sample point. The sample solution was contained in a 10 mm NMR tube and spun with a spinning cell device to ensure that every 1 kHz pulse hit fresh portion of the solution. The probe pulse was linearly focused on the sample solution in the spinning cell by planoconvex and cylindrical lenses. The Raman scattering light was collected and focused onto the entrance slit of a Czerny-Turner configured Littrow prism prefilter (Bunkoukeiki) coupled to a single spectrograph with a focal length of 550 mm (iHR550, HORIBA Jobin Yvon) by two achromatic doublet lenses. The dispersed light was detected with a liquid nitrogen cooled CCD camera (SPEC-10:400B/LN-SN-U, Roper Scientific). The Raman shifts were calibrated with Raman bands of cyclohexane. The spectral dispersion was about $1\text{ cm}^{-1}/\text{pixel}$ on the CCD camera. The accumulation time for obtaining the spectra of PYP was 90 min.

RESULTS AND DISCUSSION

Time-Resolved UVRr Spectra of WT and Y42F PYP.

Figure 1a shows UVRr spectra of wild-type (WT) PYP probed at 236 nm. Time-resolved difference spectra were obtained by subtracting the spectrum of the pG state from the spectrum measured at each delay time. For all of the difference spectra, the Raman band of water was used as an internal standard. In the time-resolved difference spectra, negative bands were clearly observed for the Tyr vibrational bands, noted as Y8a, Y7a, Y9a, and Y1.¹¹ The negative bands represent the depletion of the

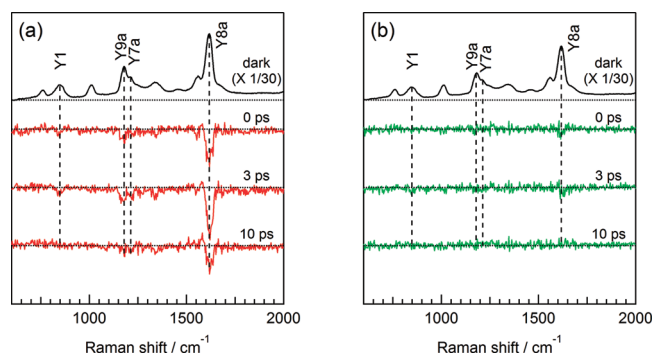


Figure 1. Picosecond time-resolved UVRr spectra of (a) WT and (b) Y42F PYP (probe 236 nm, pump 446 nm). The top trace is the probe-only spectrum divided by a factor of 30, representing the UVRr spectrum of the pG state of PYP. The spectrum of the buffer has been subtracted. The other spectra are time-resolved difference spectra generated by subtracting the probe-only spectrum from the pump–probe spectrum at each delay time.

Raman intensity due to the change in protein structure upon the formation and decay of the pG* state. The probe wavelength was located at the red side of the maximum of the Raman excitation profile of Tyr (225 nm).¹² The intensity depletion of the Tyr bands under this probe condition arises from the blue shift of the excitation profile. It has been reported that an increase in HB strength gives rise to a blue shift in the excitation profiles of Tyr UVRr bands.¹³ The depletion of the Tyr bands implies that the HB of the phenolic OH group is strengthened upon the photo-reaction of pCA.

PYP possesses five Tyr residues: Tyr42, Tyr76, Tyr94, Tyr98, and Tyr118. Tyr42 is the most probable candidate for the residue responsible for the spectral change in the WT spectra, because its phenolic OH group is directly hydrogen-bonded to pCA. To identify the Tyr residue(s) responsible for the spectral change, we compared time-resolved difference spectra of Y42F mutant to those of WT. It was known that Y42F mutant in the pG state is in the mixture of yellow ($\lambda_{\text{max}} = 458\text{ nm}$) and intermediate ($\lambda_{\text{max}} = 390\text{ nm}$) spectral forms at neutral pH,⁷ while the yellow form is dominant in WT. Since the yellow form has much larger molar extinction coefficient at the wavelength of the pump pulse (446 nm) than the intermediate form, the yellow form is predominantly excited by the pump excitation in the present time-resolved measurements, similarly to the measurements of WT. Hence, we can neglect the contribution of the intermediate spectral form. In the time-resolved difference spectra of Y42F (Figure 1b), the negative bands of the Tyr vibration almost completely disappeared. Since the lifetime of the pG* state of Y42F mutant is longer than that of WT,¹⁴ the disappearance means that the remaining four Tyr residues in Y42F mutant undergoes little structural and/or environmental changes and that Tyr42 is solely responsible for the spectral changes upon photoexcitation of pCA. Thus, we succeeded in detecting the spectral change of a single Tyr residue in PYP and concluded that the HB between pCA and Tyr42 is strengthened in the pG* state.

UVRr Spectra of Tyr42 in the pG State of WT and E46Q PYP. The HB between pCA and Glu46 is a LBHB in the pG state,⁵ while it is a normal HB in the pG* state.¹⁵ This change in the HB can result in the observed change of the HB between pCA and Tyr42 upon photoexcitation. If this is the case, substitution of Glu46 for Gln will strengthen the HB between pCA and Tyr42

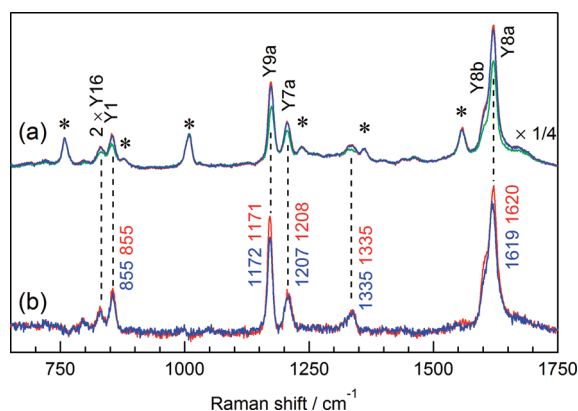


Figure 2. (a) UVRR spectra in the pG state of PYP measured by the 236 nm nanosecond pulse. The spectrum of the buffer has been subtracted. These spectra were divided by a factor of 4. (b) UVRR spectra of Tyr42 in the pG state. These spectra were obtained by subtracting the spectrum of Y42F from that of WT or E46Q. Red-, blue-, and green-colored spectra represent the spectra of WT, E46Q, and Y42F PYP, respectively. The asterisks represent Trp bands.

because the HB between pCA and Gln46 should be a normal HB in the E46Q mutant.¹⁶ We compared the UVRR spectra of Tyr42 in WT and E46Q PYP to determine structural changes in the HB network around pCA including Tyr42 in the pG state. Figure 2a shows UVRR spectra of WT, E46Q, and Y42F PYP in the pG state probed at 236 nm by using nanosecond laser pulses. Under the present condition, both the Tyr and Trp vibrational bands were predominantly observed in all the spectra. WT PYP possesses five Tyr and one Trp residues, which contribute to the UVRR spectrum of WT PYP. The single Trp residue, Trp119, is far from pCA. Even if the HB network around pCA changed, the structure of Trp119 would not change. Consequently, the Trp bands can be used as an internal standard for Raman intensity. The UVRR spectra in Figure 2a are normalized by the Trp bands.

The contribution of a Tyr residue can be masked by substitution for a Phe residue. If substitution of a Tyr residue for a Phe residue does not change the spectral features of the other Tyr residues, the contribution from the remaining four Tyr residues to the UVRR spectrum can be eliminated by subtraction of the spectrum of Y42F from that of WT.¹⁷ Thus, the spectral contribution of Tyr42 in the WT spectrum can be extracted by this subtraction. Also for E46Q mutant, the contribution of the remaining four Tyr residues to the UVRR spectrum can be eliminated by subtraction of the spectrum of Y42F from that of E46Q mutant if we assume the Y42F and E46Q substitutions do not affect the spectra of the remaining four Tyr residues.

Figure 2b shows UVRR spectra of Tyr42 in the pG state of WT and E46Q. The UVRR intensities of the Y8a, Y8b, and Y9a bands for the Tyr42 in WT were stronger than those in E46Q by $20 \pm 5\%$, suggesting that the HB between pCA and Tyr42 is strengthened by substituting Glu46 for Gln in the pG state. This is consistent with recent NMR observation that substitution of Glu46 for Gln resulted in a downfield shift in the peak position of Tyr42, suggesting that the substitution strengthened the HB between pCA and Tyr42.¹⁸

Several geometrical factors can affect the HB strength between pCA and Tyr42 in the pG state. X-ray crystallographic data show that the distance between the phenolic oxygen of pCA and the

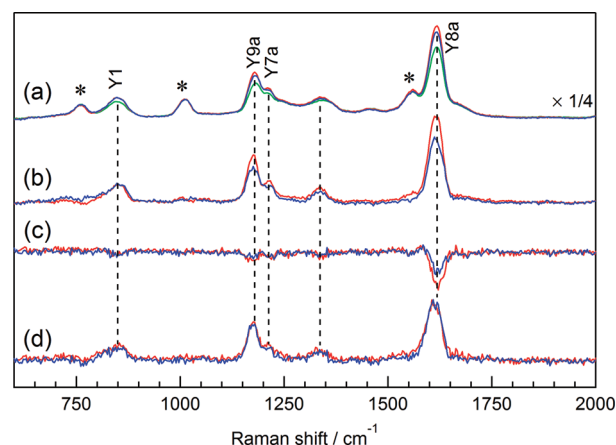


Figure 3. (a) UVRR spectra in the pG state of PYP measured by using the 236 nm picosecond pulse. The spectrum of the buffer has been subtracted. These spectra were divided by a factor of 4. (b) UVRR spectra of Tyr42 in the pG state. These spectra were obtained by subtracting the spectrum of Y42F from that of WT or E46Q. (c) Time-resolved UVRR difference spectra measured at 3 ps of the WT and E46Q (pump 446 nm, 25 μ J; probe 236 nm, 0.5 μ J). (d) UVRR spectra of Tyr42 in the pG* state. Red-, blue-, and green-colored spectra represent the spectra of WT, E46Q, and Y42F PYP, respectively. The asterisks represent Trp bands.

phenolic oxygen of Tyr42 is 2.48 Å in E46Q, whereas it is 2.50 Å in WT.^{16,19} Thus, it is possible that the distance between pCA and Tyr42 becomes slightly shorter upon E46Q substitution in the pG state. It is likely that the strengthening of the HB results from the change in the HB distance. In addition, interaction with the other amino acid residue(s), such as Thr50, as well as displacement of a hydrogen atom of Tyr42, can affect the HB strength. On the other hand, we cannot attribute the change of the HB strength to that of the dihedral angle formed between the COH and benzene planes in a Tyr molecule: the frequency of the Y9a band of Tyr42 in E46Q was close to that in WT, suggesting that the dihedral angle²⁰ is not affected by the substitution.

UVRR Spectra of Tyr42 in the pG* State of WT and E46Q PYP. The spectral change of Tyr42 upon photoexcitation was examined by picosecond time-resolved UVRR measurements. Figure 3c shows the time-resolved UVRR difference spectra measured at 3 ps of WT and E46Q PYP. The width of the Raman bands in Figure 3 was broadened compared with that in Figure 2 because the spectral width of the picosecond pulse was broader than that of the nanosecond pulse. We measured time-resolved spectra under the strong excitation condition (pump energy of 25 μ J), so that the spectral change associated with the photoexcitation was saturated. This implies that all the photoreactive molecules are excited to the pG* state. At the present pump wavelength, the absorbance of E46Q is nearly equal to that of WT. This implies that the yield of the photoexcitation of E46Q is almost the same as that of WT and that the amplitude of the spectral change upon the photoreaction reflects the difference of the HB strength between the pG* and pG states for WT and E46Q. The spectral changes observed in the time-resolved difference spectra are solely ascribed to the change in Tyr42 as we mentioned for Figure 1. Figure 3c shows that the UVRR spectral change of Tyr42 in E46Q is smaller than that in WT. This indicates that the change in the HB strength between pCA and Tyr42 for E46Q is smaller than that for WT upon the photoexcitation. The UVRR spectra of the pG state indicated

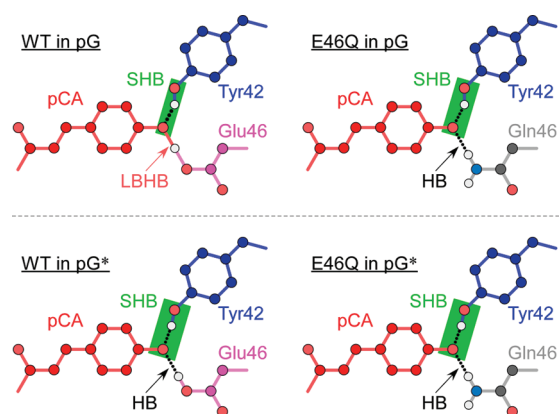


Figure 4. Changes in HB network around pCA in the pG (top) and pG* (bottom) states of WT and E46Q PYP. Green squares indicate the SHB between pCA and Tyr42. The widths of the rectangles represent the HB strength of the SHB.

that HB strength between pCA and Tyr42 for E46Q is stronger than that for WT as shown (Figure 2). The time-resolved UVR spectra of WT showed that the HB becomes stronger upon the photoexcitation of the pG state to the pG* state (Figure 1). Thus, it is suggested that the difference in the pCA•Tyr42 HB strength between WT and E46Q becomes smaller upon the formation of the pG* state.

We obtained UVR spectra of Tyr42 in the pG* state of WT and E46Q as follows, to compare the HB strength between pCA and Tyr42 for WT and E46Q. Figure 3a shows UVR spectra of WT, E46Q, and Y42F PYP measured using picosecond laser pulses. These spectra in Figure 3a contain all the Tyr bands in the molecule. First, we extracted the UVR spectra of Tyr42 in the pG state of WT and E46Q as shown in Figure 3b, by using the subtraction method in Figure 2. Similarly to Figure 2, it was observed that Y8a, Y8b, and Y9a bands for the Tyr42 in E46Q were weaker than those in WT, indicating that the HB between pCA and Tyr42 in E46Q is stronger than that in WT. Next, we calculated the spectral changes of Tyr42 upon the photoexcitation from the pG to pG* state. By using polarized light, one-third of the molecules are photoexcited for isotropic samples under the saturated condition, because the isotropic bulk sample absorbs one-third as much light as samples of molecules that are aligned parallel to the light polarization. Therefore, the putative difference spectra of Tyr42 between the pG* and pG states can be calculated by dividing the time-resolved difference spectra at 3 ps measured under the strong excitation by one-third. The spectra of the pG state (trace 3b) were added to the difference spectra between the pG and pG* states (trace 3c), to obtain the UVR spectra of Tyr42 in the pG* state of WT and E46Q as shown in Figure 3d. The band intensities of Tyr42 in E46Q are close to those in WT. This suggests that the HB strength between pCA and Tyr42 in E46Q is comparable to that in WT in the pG* state, in contrast to the case of the pG state. This contrast is reasonable because the HB between pCA and Glu46 is normal in the pG* state for both WT and E46Q, while it is a LBHB and a normal HB for WT and E46Q, respectively, in the pG state. It was reported that substitution of Glu46 for Gln did not significantly affect the lifetime of the pG* state despite the fact that Y42F and E46A mutants exhibited acceleration in the decay of the pG* state.¹⁴ This would be because the two HBs formed by pCA are similar between WT and E46Q in the pG* state.

It should be pointed out that a pronounced band was observed at 1335 cm^{-1} in the UVR spectra of Tyr42 in the pG state for both WT and E46Q. This band was also observed in the pG* state spectra of WT and E46Q PYP. On the other hand, the intensity of this band was not enhanced in the UVR spectrum of Tyr in aqueous solution.¹² On the basis of the frequency, this band can be assigned to Y3 mode.²¹ To the best of our knowledge, this band has been never observed in UVR spectra of Tyr in protein, suggesting unusual environment for Tyr42 in PYP.

Figure 4 summarizes the structural changes of the HB network around pCA. In the pG state, the HB between pCA and Glu46 changes from a LBHB to a normal HB upon the substitution from Glu46 for Gln.^{5,16,22} This implies that the HB strength in E46Q is weaker than that in WT. The HB between pCA and Tyr42, on the other hand, remains a SHB in both the crystal structures of WT and E46Q.⁴ The present UVR study revealed that the HB of Tyr42 becomes stronger upon substitution of Glu46. In the pG* state, the UVR data indicated that the HB network around pCA was not altered upon substitution of Glu46 for Gln. The results described above show that the two HBs formed by pCA correlate with each other in the network. The substitution of Glu46 for Gln makes the HB between pCA and the residue at the 46th position weaker in the pG state, resulting in a stronger HB between pCA and Tyr42. This is consistent with recent reports on the coupling of the two HBs in the pG state.^{18,23} In the pG* state, on the other hand, as the HB between pCA and Glu46 is a normal HB even in WT, the substitution of Glu46 for Gln induces little change to the HB between pCA and the residue at the 46th position. As a result, the substitution does not change the HB strength between pCA and Tyr42.

Quantum chemical calculations revealed that HBs of the phenolic oxygen of pCA to Tyr42 and Glu46 have a strong effect on the low-lying excited states of the chromophore.²⁴ The HBs give rise to pronounced energetic shifts of the electronic state. Therefore, it is highly likely that the observed change of the HBs of pCA upon the pG* formation affects a potential energy surface of the electronic excited state and thus could promote the photoisomerization of pCA. In fact, the E46Q mutant showed a similar rate for isomerization with WT, whereas Y42F and E46A mutants showed slower rate for isomerization than WT.¹⁴ This indicates that elimination of one of the two HBs affects the rate for isomerization. We speculate that the change of the HBs of pCA upon the pG* formation helps pCA to isomerize efficiently.

To conclude, we elucidated the structure of the HB network around pCA in the pG and pG* states based on the spectral contribution of Tyr42. In the pG state, the HB between pCA and Tyr42 in WT is weaker than that in E46Q. In the pG* state, the HB network around pCA of WT is similar to that of E46Q. To date, protein structures in the excited state have been less well characterized. The present UVR study provides new insights into the dynamics of the HB network around pCA of PYP, which will lead to a greater understanding of the signal transduction mechanism.

AUTHOR INFORMATION

Corresponding Author

*Phone: +81-6-6850-5776. Fax: +81-6-6850-5776. E-mail: mztan@chem.sci.osaka-u.ac.jp.

■ ACKNOWLEDGMENT

This work was supported by a Grant-in-Aid for Scientific Research on the Priority Area Molecular Theory for Real Systems (Grant No. 20038037) from the Ministry of Education, Culture, Sports, Science and Technology of Japan (MEXT) to M.M., and a Grant-in-Aid for Scientific Research on the Priority Area Molecular Science for Supra Functional Systems (Grant No. 19056013) from MEXT to Y.M.

■ REFERENCES

- (1) Sprenger, W. W.; Hoff, W. D.; Armitage, J. P.; Hellingwerf, K. J. *J. Bacteriol.* **1993**, *175*, 3096.
- (2) Ujj, L.; Devanathan, S.; Meyer, T. E.; Cusanovich, M. A.; Tollin, G.; Atkinson, G. H. *Biophys. J.* **1998**, *75*, 406.
- (3) Groot, M. L.; Wilderen, L. J. G. W. v.; Larsen, D. S.; Horst, M. A. v. d.; Stokkum, I. H. M. v.; Hellingwerf, K. J.; Grondelle, R. v. *Biochemistry* **2003**, *42*, 10054.
- (4) Anderson, S.; Crosson, S.; Moffat, K. *Acta Crystallogr. Sect. D, Biol. Crystallogr.* **2004**, *60*, 1008.
- (5) Yamaguchi, S.; Kamikubo, H.; Kurihara, K.; Kuroki, R.; Niiumura, N.; Shimizu, N.; Yamazaki, Y.; Kataoka, M. *Proc. Natl. Sci. Acad. Sci. U.S.A.* **2009**, *106*, 440.
- (6) Mizuno, M.; Hamada, N.; Tokunaga, F.; Mizutani, Y. *J. Phys. Chem. B* **2007**, *111*, 6293.
- (7) Mihara, K. i.; Hisatomi, O.; Inamoto, Y.; Kataoka, M.; Tokunaga, F. *J. Biochem.* **1997**, *121*, 876.
- (8) Sato, A.; Mizutani, Y. *Biochemistry* **2005**, *44*, 14709.
- (9) Tauber, M. J.; Mathies, R. A.; Chen, X.; Bradforth, S. E. *Rev. Sci. Instrum.* **2003**, *74*, 4958.
- (10) Kaminaka, S.; Mathies, R. A. *Appl. Spectrosc.* **1998**, *52*, 469.
- (11) Harada, I.; Takeuchi, H. Raman and Ultraviolet Resonance Raman Spectra of Proteins and Related Compounds. In *Spectroscopy of Biological Systems*; Clark, R. J. H., Hester, R. E., Eds.; John Wiley & Sons: Chichester, UK, 1986; p 113.
- (12) Ludwig, M.; Asher, S. A. *J. Am. Chem. Soc.* **1988**, *110*, 1005.
- (13) Chi, Z.; Asher, S. A. *J. Phys. Chem. B* **1998**, *102*, 9595.
- (14) Devanathan, S.; Lin, S.; Cusanovich, M. A.; Woodbury, N.; Tollin, G. *Biophys. J.* **2001**, *81*, 2314.
- (15) Heyne, K.; Mohammed, O. F.; Usman, A.; Dreyer, J.; Nibbering, E. T. J.; Cusanovich, M. A. *J. Am. Chem. Soc.* **2005**, *127*, 18100.
- (16) Sugishima, M.; Tanimoto, N.; Soda, K.; Hamada, N.; Tokunaga, F.; Fukuyama, K. *Acta Crystallogr. Sect. D, Biol. Crystallogr.* **2004**, *60*, 2305.
- (17) The chromophores of the yellow and intermediate forms of Y42F are in partially deprotonated and protonated states, respectively. It is likely that there is little difference between UVR spectra of the remaining four Tyr residues for the yellow and intermediate forms because the Tyr residues exhibited little difference between UVR spectra of pG and pG* states as shown in Figure 1. The change in the electronic distribution of the chromophore does not affect UVR spectra of the remaining four Tyr residues.
- (18) Sigala, P. A.; Tsuchida, M. A.; Herschlag, D. *Proc. Natl. Acad. Sci. U.S.A.* **2009**, *106*, 9232.
- (19) Anderson, S.; Srajer, V.; Pahl, R.; Rajagopal, S.; Schotte, F.; Anfinsen, P. A.; Wulff, M.; Moffat, K. *Structure* **2004**, *12*, 1039.
- (20) Takeuchi, H.; Watanabe, N.; Sato, Y.; Harada, I. *J. Raman Spectrosc.* **1989**, *20*, 233.
- (21) Takeuchi, H.; Watanabe, N.; Harada, I. *Spectrochim. Acta* **1988**, *44A*, 749.
- (22) Anderson, S.; Crosson, S.; Moffat, K. *Acta Crystallogr. Sect. D, Biol. Crystallogr.* **2004**, *60*, 1008.
- (23) Joshi, C. P.; Otto, H.; Hoersch, D.; Meyer, T. E.; Cusanovich, M. A.; Heyn, M. P. *Biochemistry* **2009**, *48*, 9980.
- (24) Gromov, E. V.; Burghardt, I.; Köppel, H.; Cederbaum, L. S. *J. Am. Chem. Soc.* **2007**, *129*, 6798.